Effects of biaxial strain on the intervalence-band absorption spectra of InGaAs/InP systems

A. Afzali-Kushaa[a] and G. I. Haddad
Solid-State Electronics Laboratory, Department of Electrical Engineering and Computer Science, The University of Michigan, Ann Arbor, Michigan 48109

(Received 12 December 1994; accepted for publication 17 February 1995)

The effects of biaxial strain on the intervalence-band absorption spectra of p-doped InGaAs/InP bulk layers are investigated. The study is performed by calculating and comparing the absorption coefficients corresponding to the direct transitions between the heavy and light hole bands, between the heavy hole and split-off bands, and between the split-off and light hole bands in both the lattice matched and the strained layers. The valence-band structures of these layers are neither isotropic nor parabolic and hence the $\mathbf{k}\cdot\mathbf{p}$ approach is utilized to calculate the band structures and their corresponding wave functions. The quantities are then invoked in the calculation of the (joint) density of states, the Fermi energy, and the momentum matrix element, which are needed in the evaluation of the intervalence-band absorption coefficients. These calculated results show that the intervalence-band absorption coefficients depend on the strain in the layer. The dependence is determined by the bands involved in the intervalence transition, the polarization of the incident light, and the type of the strain (compressive or tensile). © *1995 American Institute of Physics.*

I. INTRODUCTION

The intervalence-band absorption coefficients have been measured and calculated for elemental and compound semiconductors.[1–10] These studies, however, are only concerned with lattice matched or uniaxially strained layers. Within the last decade, epitaxial growth techniques such as molecular-beam epitaxy and chemical beam epitaxy have improved to the point where very high quality semiconductor films composed of materials with a different lattice constant than that of the substrate may be controllably grown. The grown layer will be either under biaxial tensile strain, if the lattice constant of the grown layer is larger than the substrate lattice constant, or under biaxial compressive strain, if the substrate lattice constant is larger than that of the layer. The thickness of the strained layer, however, may not exceed a certain thickness called the critical thickness for the pseudomorphic or coherent layer, i.e., a layer without an unacceptable number of dislocations. The thickness is inversely proportional to the strain in the layer. One of the primary effects of the strain (uniaxial or biaxial) on band structure is to lift band-structure degeneracies, through symmetry breaking. Therefore the light and heavy hole band minima are not degenerate in these layers where the energy difference between them is proportional to the strain in the system. If the applied strain is small (small lattice mismatch between the layer and the substrate), the Brillouin-zone-center energy separation falls in the far-infrared (FIR) frequency range which suggests the possibility of using these layers in FIR sources and detectors. The FIR emission has been recently observed from uniaxially strained p-Ge bulk layers.[11] To investigate the possible application of the biaxially strained layers in FIR detectors and sources,[12] one needs to determine the intervalence-band absorption coefficients.

In this work, we will investigate the effects of the biaxial strain on the intervalence-band absorption spectra by calculating and comparing the absorption coefficients for both the p-type doped lattice matched and strained InGaAs/InP structures. In addition to the intervalence-band absorption (direct transition), there are other absorption mechanisms such as the free-carrier absorption (indirect transition) which could be important in bulk layers in the frequency range of the results presented. To calculate the total absorption coefficient, the absorption coefficient due to these mechanisms should also be calculated and added to the intervalence-band absorption coefficients presented in this work. The focus of this paper, however, is only on the intervalence-band absorption coefficients. The structures under study include the lattice matched layer $In_{0.53}Ga_{0.47}As/InP$, the tensile strained layer $In_{0.49}Ga_{0.51}As/InP$ with 0.29% lattice mismatch, and the compressively strained layer $In_{0.58}Ga_{0.42}As/InP$ with 0.33% lattice mismatch. The zone-center energy separations in both strained systems are about 20 meV, with the critical thickness about 0.1 μm, which is adequate for the thickness of a layer with bulk properties. In Sec. II, first the formulation used in the calculation of the valence-band structure is given and then the band structures of the layers are presented and discussed. The calculated oscillator strengths for different intervalence-band transitions are presented in Sec. III while the procedure used in determining the momentum matrix elements from the $\mathbf{k}\cdot\mathbf{p}$ method is also described in this section. The intervalence-band absorption coefficients for these layers are presented and discussed in Sec. IV. Finally, the summary is given in Sec. V.

II. VALENCE-BAND STRUCTURE

In this work, we are primarily interested in the *optical* properties of the semiconductors and hence the band structure around the center of the Brillouin zone is needed for this type of calculation. This allows us to invoke the $\mathbf{k}\cdot\mathbf{p}$ method

[a]Electronic mail: afzali@engin.umich.edu

 0021-8979/95/77(12)/6549/8/$6.00

which is based on perturbation theory. The band structure and the wave functions for holes may be calculated based on this approach where a set of coupled multiband effective-mass equations are solved.[2,13] The valence-band structure at the Brillouin-zone center, in the absence of the spin-orbit splitting, is sixfold degenerate, corresponding to the three p functions times the two spin functions, spin up and spin down. The zone-center Bloch functions ($u_{J,\pm j}$) are the angular momentum states corresponding to the so-called heavy hole (HH) $u_{3/2,\pm 3/2}$, light hole (LH) $u_{3/2,\pm 1/2}$, and split-off (SO) $u_{1/2,\pm 1/2}$ bands, all with the same energy E_0, neglecting the spin-orbit splitting. Spin-orbit splitting partially removes this degeneracy by lowering the two $J=1/2$ bands (split-off bands) with respect to the four $J=3/2$ bands (heavy and light hole bands). In the $\mathbf{k}\cdot\mathbf{p}$ method, the wave function for band n may be written in the following vector notation:

$$\psi^n = e^{i\mathbf{k}\cdot\mathbf{r}}(\mathbf{F}^n)^T\mathbf{U}, \tag{1}$$

where

$$\begin{aligned}\mathbf{U}&=[u_{3/2,3/2}\quad u_{3/2,1/2}\quad u_{3/2,-1/2}\quad u_{3/2,-3/2}\\&\quad\times u_{1/2,1/2}\quad u_{1/2,-1/2}]^T,\\ \mathbf{F}^n&=[f^n_{3/2,3/2}\quad f^n_{3/2,1/2}\quad f^n_{3/2,-1/2}\quad f^n_{3/2,-3/2}\\&\quad\times f^n_{1/2,1/2}\quad f^n_{1/2,-1/2}]^T.\end{aligned} \tag{2}$$

Here $\mathbf{k}$ and $\mathbf{r}$ represent the position in phase and real space and $f^n_{J,j}(\mathbf{k})$ are the weighting factors (the superscript n denotes different bands). In the $\mathbf{k}\cdot\mathbf{p}$ method, the second-order energy change $E^n(\mathbf{k})$ in the degenerate states and the vector $\mathbf{F}^n$ may be obtained from the solution of the following secular equation:

$$[\mathbf{H}(\mathbf{k})-E^n(\mathbf{k})]\mathbf{F}^n(\mathbf{k})=0. \tag{3}$$

The matrix is given by[13,14]

$$\mathbf{H}(\mathbf{k})=\begin{bmatrix} H_{\rm hh} & b & c & 0 & ib/\sqrt{2} & -i\sqrt{2}c \\ b^\dagger & H_{\rm lh} & 0 & c & -iq & i\sqrt{3}b/\sqrt{2} \\ c^\dagger & 0 & H_{\rm lh} & -b & -i\sqrt{3}b^\dagger/\sqrt{2} & -iq \\ 0 & c^\dagger & -b^\dagger & H_{\rm hh} & -i\sqrt{2}c^\dagger & -ib^\dagger/\sqrt{2} \\ -ib^\dagger/\sqrt{2} & iq & i\sqrt{3}b/\sqrt{2} & i\sqrt{2}c & H_{\rm so} & 0 \\ i\sqrt{2}c^\dagger & -i\sqrt{3}b^\dagger/\sqrt{2} & iq & ib/\sqrt{2} & 0 & H_{\rm so} \end{bmatrix}, \tag{4}$$

where

$$\begin{aligned} H_{\rm hh}&=\frac{\hbar^2}{2m_0}[(k_x^2+k_y^2)(\gamma_1+\gamma_2)+(\gamma_1-2\gamma_2)k_z^2],\\ H_{\rm lh}&=\frac{\hbar^2}{2m_0}[(k_x^2+k_y^2)(\gamma_1-\gamma_2)+(\gamma_1+2\gamma_2)k_z^2],\\ H_{\rm so}&=\frac{H_{\rm hh}+H_{\rm lh}}{2}+\Delta_0,\quad b=-\frac{\sqrt{3}\hbar^2}{m_0}\gamma_3(k_yk_z+ik_xk_z),\\ c&=\frac{\sqrt{3}\hbar^2}{2m_0}[\gamma_2(k_x^2-k_y^2)-2i\gamma_3k_xk_y],\quad q=\frac{H_{\rm hh}-H_{\rm lh}}{\sqrt{2}}. \end{aligned} \tag{5}$$

Here m_0 is the free-electron mass, $\hbar$ the reduced Planck's constant, and γ_1, γ_2, and γ_3 the Kohn–Luttinger parameters.

To calculate the band structure of the other two layers which are under strain, one needs to incorporate the effect of the strain in the $\mathbf{k}\cdot\mathbf{p}$ Hamiltonian. To include the effect of the strain in the calculation of the band structure, the Hamiltonian in Eq. (3) is modified by adding the strain perturbing Hamiltonian[15] which is found using the deformation potential approximation. The strain perturbing Hamiltonian in the angular momentum basis is obtained by utilizing the following recipe. Assuming that the matrix has the same elements as given in the matrix in Eq. (4), except for the superscript ϵ, the matrix elements of the strain perturbing Hamiltonian are found from the equations in Eq. (13) by replacing γ_1, γ_2, γ_3, and k_ik_j by a, $b/2$, $d/2\sqrt{3}$, and ϵ_{ij}, respectively. We should also set $\hbar^2/2m_0=1$ and $\Delta_0=0$. Therefore we can write[15]

$$\begin{aligned} H^\epsilon_{\rm hh}&=\left(\frac{2a+b}{2}\right)(\epsilon_{xx}+\epsilon_{yy})+(a-b)\epsilon_{zz},\\ H^\epsilon_{\rm lh}&=\left(\frac{2a-b}{2}\right)(\epsilon_{xx}+\epsilon_{yy})+(a+b)\epsilon_{zz},\\ H^\epsilon_{\rm so}&=\frac{H^\epsilon_{\rm hh}+H^\epsilon_{\rm lh}}{2},\quad b^\epsilon=-d(\epsilon_{yz}+i\epsilon_{xz}),\\ c^\epsilon&=\frac{\sqrt{3}b}{2}(\epsilon_{xx}-\epsilon_{yy})-id\epsilon_{xy},\\ q^\epsilon&=\frac{H^\epsilon_{\rm hh}-H^\epsilon_{\rm lh}}{\sqrt{2}}. \end{aligned} \tag{6}$$

In a strained layer grown along the (001) direction, which will be the structure of our interest, we have[13]

$$\begin{aligned} \epsilon_{xx}&=\epsilon_{xx}=\frac{a_{\rm substrate}}{a_{\rm layer}}-1\equiv\epsilon,\quad \epsilon_{zz}=-2\,\frac{c_{12}}{c_{11}}\,\epsilon,\\ \epsilon_{xy}&=\epsilon_{xz}=\epsilon_{yz}=0, \end{aligned} \tag{7}$$

where $a_{\rm layer}$ and $a_{\rm substrate}$ are the layer and substrate lattice constants, respectively, and c_{11},c_{12} are the elastic stiffness constants.

Having found the total Hamiltonian which includes the effect of the strain, we can calculate the band structure for all

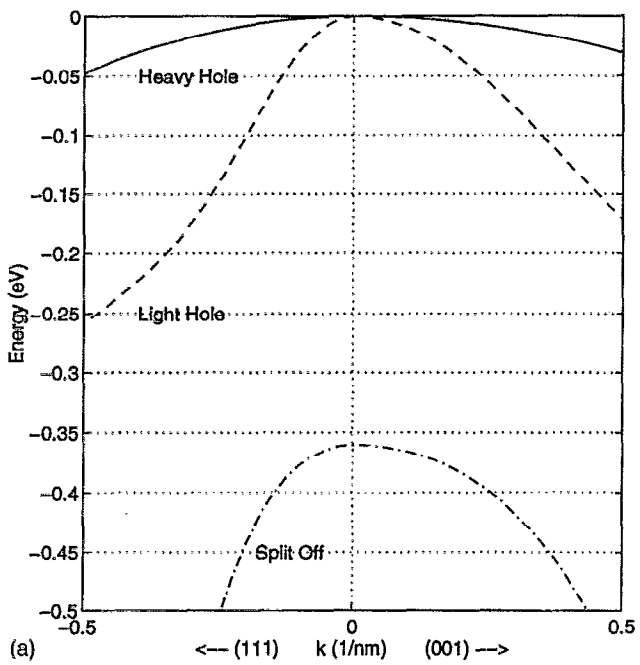

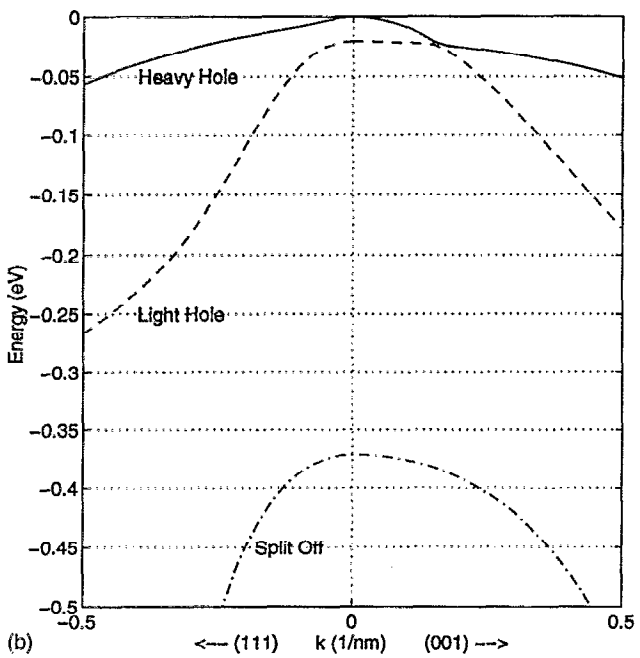

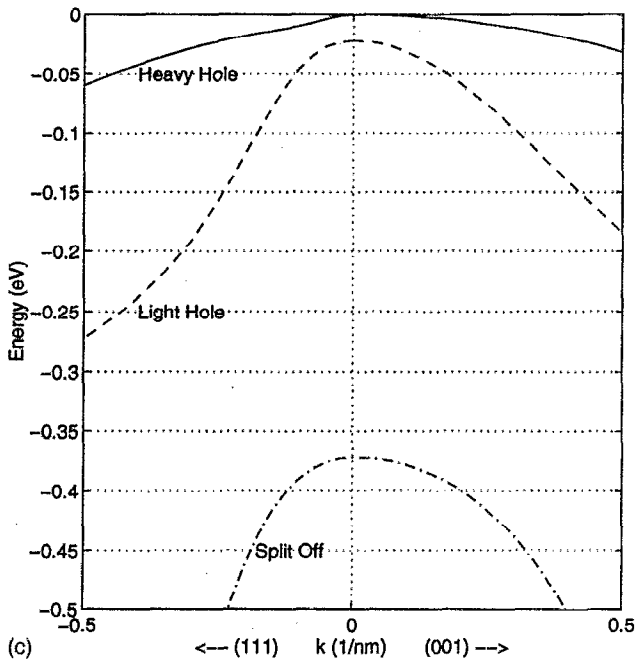

FIG. 1. Band structure of (a) $In_{0.53}Ga_{0.47}As$ layer (latticed matched), (b) $In_{0.49}Ga_{0.51}As$ layer (tensile strain), and (c) $In_{0.58}Ga_{0.42}As$ layer (compressive strain) calculated using $\mathbf{k}\cdot\mathbf{p}$ approach.

three layers. We have plotted the band structure along the (001) and (111) directions for these layers in Fig. 1. The band structure of the $In_{0.53}Ga_{0.47}As$ layer is shown in Fig. 1(a). The degeneracy of the two lower bands, so-called heavy and light hole bands, is evident in the figure. As can be observed from the figure, the band structure is neither isotropic nor parabolic for any of the three bands (six bands including the spin degeneracy factor) and therefore may not be approximated by a single effective mass. In Fig. 1(b) and 1(c), the band structure for the layers under tensile strain, $In_{0.49}Ga_{0.51}As$, and under compressive strain, $In_{0.58}Ga_{0.42}As$, are shown where the lattice mismatch for the first layer is about 0.29% while for the second layer is about 0.31%. Here, again, the band structures are neither isotropic nor parabolic and therefore cannot be modeled by single effective-mass bands. As is evident from the figures, the degeneracy of the light and heavy hole bands are lifted in these two layers. The energy separation at the zone center for both cases is about 20 meV. Since the symmetry of each band changes with the wave vector, in this work for convenience we call the band on top of the valence band the heavy hole band and the next band is called light hole band. In the case of the tensile strained layer [see Fig. 1(b)] the band called the heavy hole band here has a smaller effective mass along the (001) direction.

In the case of the compressively strained layer the mini-

mum energy separation between the heavy and light hole bands is greater than zero (about 20 meV) which, as we will see later, will lead to zero intervalence-band absorption coefficient for energies less than this minimum energy difference. This is not the case for the tensile strained layer where the energy separation between the heavy and light hole bands decreases and finally reaches zero as the magnitude of the wave vector along the (001) direction increases. Also note that at the zone center the energy separation between the split-off and heavy hole bands is about 0.36 eV, in the case of the lattice matched layer, and about 0.37 eV, in the case of strained layers. The split-off–light hole band joint density of states in all three cases is nonzero for energies less than 0.36 eV.[16] The split-off–light hole band joint density of states was higher than the split-off–heavy hole band joint density of states in the range of our calculations which originates from the fact that the two bands become almost parallel in some directions in phase space. As will be discussed later, the absorption coefficient is proportional to the joint density of states as well as the difference between the occupation factor of the initial and final states. Although the joint density of states is higher for the split-off to light hole transition, the intervalence-band absorption coefficient for this transition is lower, especially at low hole concentrations and temperatures.[16] This is because the electronic states of the light hole band reside at lower energies and therefore are mostly filled with electrons, leading to very small differences in the occupation factor and hence smaller absorption coefficients for this transition.

III. MOMENTUM MATRIX ELEMENTS

The intervalence-band radiative transition rate and therefore the absorption and gain coefficients depend on the intervalence momentum matrix elements. For band n to n' transition, the momentum matrix element $\mathbf{P}_{nn'}(\mathbf{k})$ is given by[17]

$$\begin{aligned}\mathbf{a}\cdot\mathbf{P}^{nn'}(\mathbf{k}_\rho)&=\langle\psi^n(\mathbf{k},\mathbf{r})|\mathbf{a}\cdot\hat{\mathbf{p}}|\psi^{n'}(\mathbf{k},\mathbf{r})\rangle\\&=[(\mathbf{F}^n)^T]^*\langle e^{i\mathbf{k}\cdot\mathbf{r}}\mathbf{U}|\mathbf{a}\cdot\hat{\mathbf{p}}|e^{i\mathbf{k}\cdot\mathbf{r}}\mathbf{U}\rangle\mathbf{F}^{n'}\\&=[(\mathbf{F}^n)^T]^*\mathbf{P}\mathbf{F}^{n'},\end{aligned}\tag{8}$$

where $\mathbf{a}$ is the polarization unit vector—which is $\hat{\mathbf{x}}$ in the case of the x polarization and $\hat{\mathbf{z}}$ in the case of the z polarization—and the elements of $\mathbf{P}$ are given by

$$\mathbf{P}(J_1,j_1;J_2,j_2)=\langle e^{i\mathbf{k}\cdot\mathbf{r}}u_{J_1,j_1}|\mathbf{a}\cdot\hat{\mathbf{p}}|e^{i\mathbf{k}\cdot\mathbf{r}}u_{J_2,j_2}\rangle.\tag{9}$$

The procedure to calculate the momentum matrix elements from the $\mathbf{k}\cdot\mathbf{p}$ approach—which is consistent with the band-structure calculation—is as follows:[16] We assume that $\mathbf{P}$ has the same matrix elements as the matrix in Eq. (12). For any given polarization, say x, first, multiply the RHSs of the equations in Eq. (13) by $m_0/\hbar$; then, only keep the terms that have the k component along that polarization. For the x polarization keep terms with a k_x component; in the next step, divide the remaining terms by the same k component (k_x in our example). Finally, the terms that still have that k component (k_x in our example) must be multiplied by 2. Using this procedure, the momentum matrix element for all three polarizations can be calculated by adding all the elements of the matrix $\mathbf{P}$. Due to the spin degeneracy there are two different wave functions, one for spin up and one for spin down for each band at any point in phase space. The average momentum matrix element is therefore calculated for all four combinations, two states for the initial band and two states for the final band, and their sum is divided by 2 to average over the initial eigenstates.

To compare the momentum matrix element in the lattice matched and strained layers, we will calculate the oscillator strength which is a dimensionless quantity usually used to show the strength of the transition and is defined by

$$\mathrm{OS}_{nn'}(\mathbf{k})\equiv\frac{2|\mathbf{a}\cdot\tilde{\mathbf{P}}_{nn'}(\mathbf{k})|^2}{m_0|E^n(\mathbf{k})-E^{n'}(\mathbf{k})|},\tag{10}$$

where $\tilde{\mathbf{P}}_{nn'}(\mathbf{k})$ is the average momentum matrix element between bands n and n'. The oscillator strength is more meaningful than the momentum matrix element because the strength of the radiative transition is not only proportional to the matrix element but also it depends inversely upon the frequency of the photon. In Fig. 2, we have plotted the oscillator strengths for the intervalence-band transitions between the light and heavy hole bands, between the split-off and heavy hole bands, and between the split-off and light hole bands. In the case of the lattice matched and compressively strained layers and along the (001) direction where the heavy hole band has nonzero components only for the Bloch function $u_{3/2,\pm3/2}$, the transitions from the split-off and light hole bands to the heavy hole band are forbidden for the z polarization. However, the transition between the split-off and light hole bands along the (001) direction is allowed. In the case of the tensile strained layer, there is a symmetry change along this direction[16] which leads to a different selection rule. In addition, there is a discontinuity along the (001) direction for the light to heavy hole transition because the two bands merge at this point leading to zero energy difference in the denominator of Eq. (10).

IV. INTERVALENCE-BAND ABSORPTION COEFFICIENTS

The intervalence absorption coefficient due to the radiative transition between band n and n' (for example, n and n' correspond to light and heavy hole bands) is given by[17]

$$\begin{aligned}\alpha_{nn'}(\omega)=&\frac{4\pi^2e^2}{\sqrt{\epsilon_1}m_0^2\omega c}\sum_{\mathbf{k}}[f(E^n)-f(E^{n'})]\\&\times|\mathbf{a}\cdot\tilde{\mathbf{P}}_{nn'}(\mathbf{k})|^2\delta[\hbar\omega-(E^{n'}-E^n)],\end{aligned}\tag{11}$$

where ϵ_1 is the dielectric constant, e the electric charge, ω the frequency, c the light velocity in vacuum, $f(E^n)$ the occupation probability for states with energy E^n, $\mathbf{a}$ the polarization unit vector, and $\tilde{\mathbf{P}}_{nn'}(\mathbf{k})$ the average momentum matrix element between bands n and n'. As the equation suggests, the intervalence absorption coefficient depends on the occupation factor of the initial and final states. This factor is obtained from the Fermi–Dirac distribution which is a function of the Fermi energy and the temperature. The Fermi energy is a function of the density of states and the doping which determines the hole concentration. The calculations

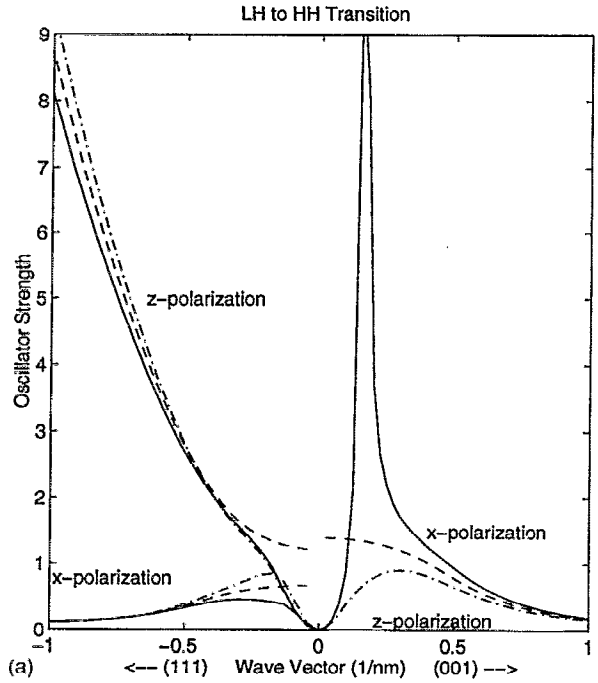

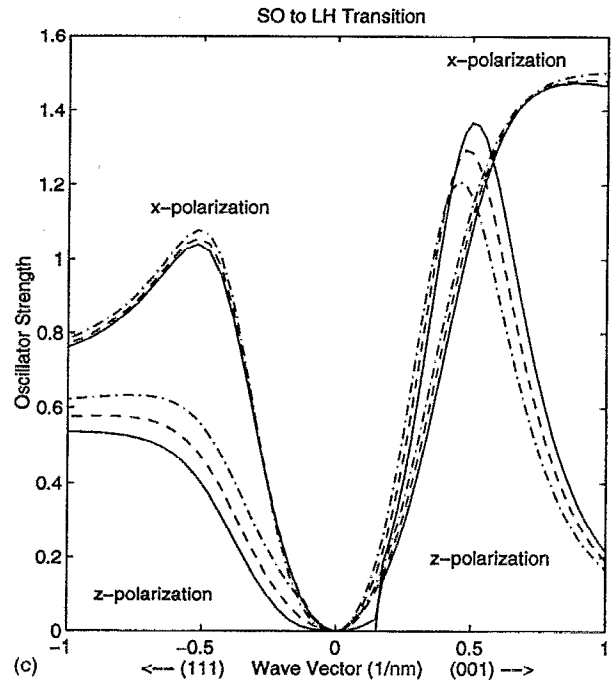

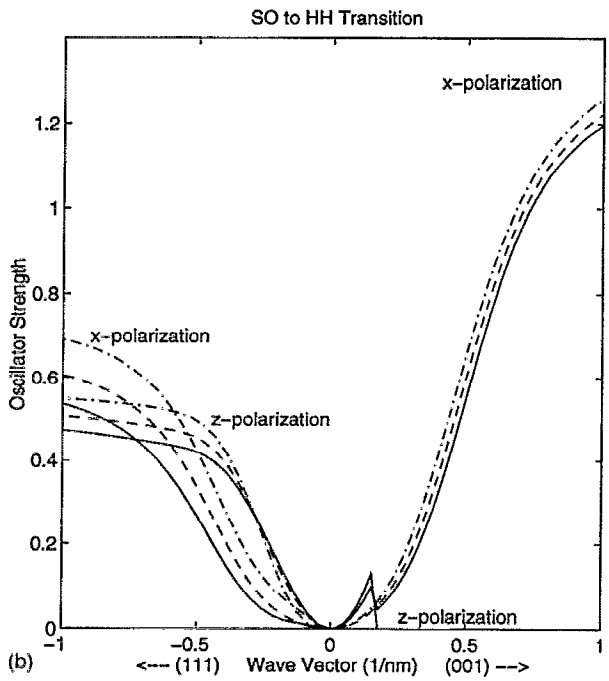

FIG. 2. Oscillator strength for the transition between (a) the heavy and light hole bands, (b) the split-off and heavy hole bands, and (c) the split-off and light hole bands. Solid, dash, and dash–dot lines correspond to tensile strained, lattice matched, and compressively strained layers, respectively.

are performed for a lattice temperature of 300 K with hole concentrations of 10^{17}, 10^{18}, and 10^{19} cm^{-3}. The corresponding doping levels for these free-hole concentrations can be determined from the doping ionization energy—which is different for different doping species—and the level of doping. The band structure of the valence band in the layers of our interest is neither parabolic nor isotropic and therefore the density of states is calculated numerically.

To make the expression more suitable for numerical evaluation, the delta-function property is employed. Hence we utilize the expression for the joint density of states which includes the matrix element and the occupation factor at each surface element corresponding to the photon energy $\hbar\omega = E^{n'} - E^{n}$, namely,

$$\alpha_{nn'}(\omega) = \frac{4\pi^2 e^2}{\sqrt{\epsilon_1} m_0^2 \omega c} \frac{1}{(2\pi)^3} \int [f(E^n) - f(E^{n'})] \times |\mathbf{a}\cdot\tilde{\mathbf{P}}_{nn'}(\mathbf{k})|^2 \frac{dS_{\hbar\omega}^{nn'}}{\nabla_{\mathbf{k}}^{nn'} \hbar\omega}, \tag{12}$$

where $dS_{\hbar\omega}^{nn'}$ denotes an element of area on the surface and $\nabla_k^{nn'}\hbar\omega$ is the gradient of the energy. The integration is over the entire Brillouin zone. As is evident from the equation, the

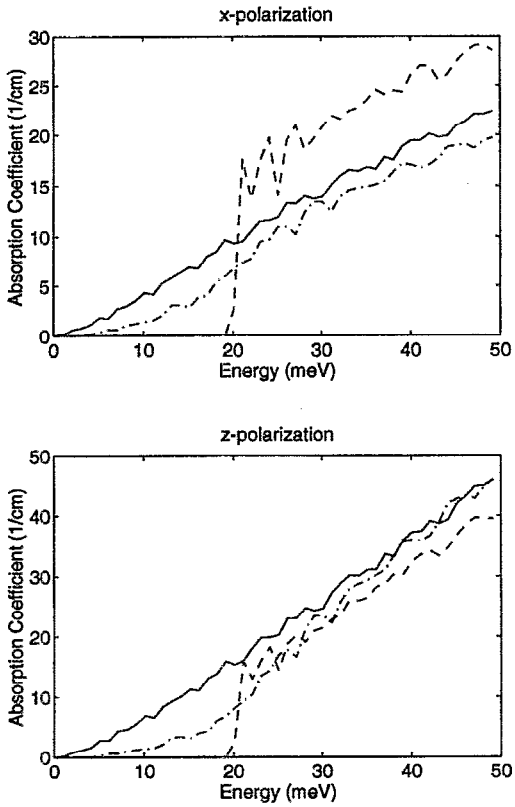

FIG. 3. Light hole band to heavy hole band absorption coefficients for 10^{17} cm^{-3} free-hole concentration at 300 K for both x and z polarizations. Solid, dash, and dash–dot lines correspond to lattice matched, compressively strained, and tensile strained layers, respectively.

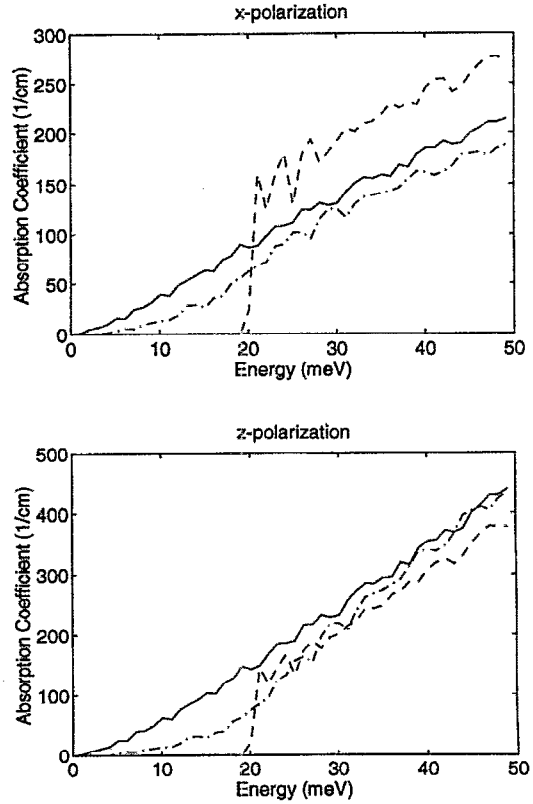

FIG. 4. Light hole band to heavy hole band absorption coefficients for 10^{18} cm^{-3} free-hole concentration at 300 K for both x and z polarizations. Solid, dash, and dash–dot lines correspond to lattice matched, compressively strained, and tensile strained layers, respectively.

intervalence absorption coefficient is proportional to the joint density of states and the momentum matrix element. It also depends on the occupation factor which is the difference between the values of the Fermi–Dirac distribution function at the energies of the initial and final bands for the same wave vector.

In the rest of this section, we present the calculated intervalence-band absorption coefficients for three different hole concentrations. The coefficients were calculated for both the x and z polarizations (the results for the y polarization are the same as those for the x polarization) and the lattice temperature was assumed to be 300 K. In the rest of the section, for convenience, we use the term "absorption coefficient" instead of the term "intervalence-band absorption coefficient." The results contain some numerical noise leading to oscillatory behavior which originates from the numerical differentiation involved in the calculation of the joint density of states.

A. Heavy to light hole transition

In Fig. 3, the absorption coefficients of all three layers with a hole concentration of 10^{17} cm^{-3} are plotted. All three coefficients increase with increasing photon energy, which is due to the fact that the Fermi energy is deep in the band gap at this temperature and hence the occupation factor does not decrease significantly with energy and cannot compensate the increase in the momentum matrix element and the joint density. As is evident from the figure, the absorption spectrum of the compressively strained layer has a low cutoff energy corresponding to the energy separation between the heavy and light hole bands at the zone center. This is not surprising because of zero joint density of states for this energy range in this layer. The absorption in the layer under tensile strain is not zero in this energy range because there are states which have transitions corresponding to these energies. However, the number of these states is smaller compared to the lattice matched case which leads to smaller joint densities of states and consequently weaker absorption at these frequencies for this layer compared to the lattice matched layer. The absorption coefficients for the z polarization are higher compared to the x-polarization case (the difference is higher for the lattice matched and tensile strained layer absorption coefficients). For the z polarization, at energies higher than the zone-center energy separation of the heavy and light hole bands, the three absorption spectra are about the same while in the case of the x polarization the absorption coefficient of the compressively strained layer is fairly higher. For the latter case, the absorption coefficient of the lattice matched layer is lower compared to the compressively strained layer and is higher compared to the tensile strained layer.

Figure 4 presents the results for the absorption coefficients when the hole concentration is 10^{18} cm^{-3}. Compared to Fig. 3, the increase in the absorption coefficients are just

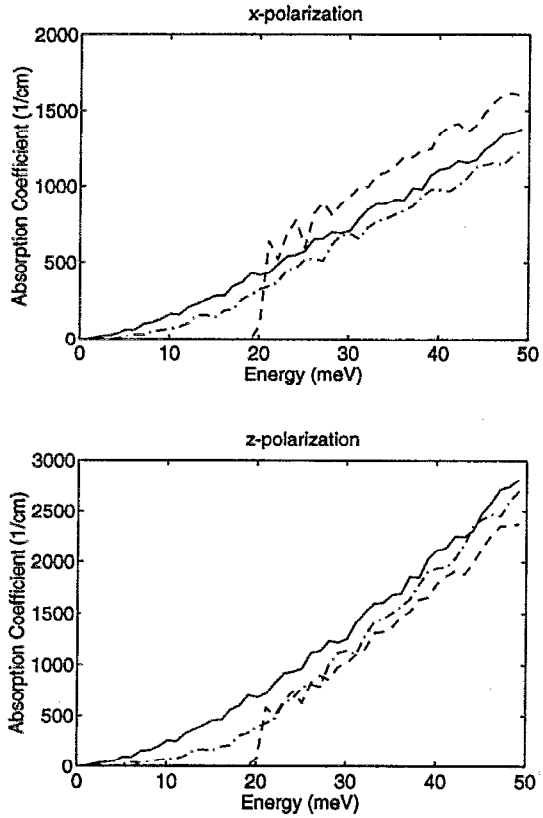

FIG. 5. Light hole band to heavy hole band absorption coefficients for 10^{19} cm^{-3} free-hole concentration at 300 K for both x and z polarizations. Solid, dash, and dash–dot lines correspond to lattice matched, compressively strained, and tensile strained layers, respectively.

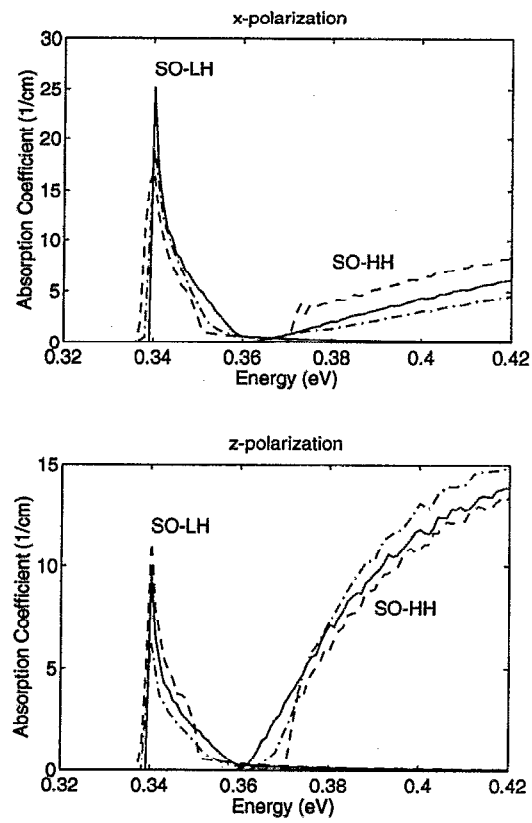

FIG. 6. Split-off band to light and heavy hole bands absorption coefficients for 10^{17} cm^{-3} free-hole concentration at 300 K for both the x and z polarizations. Solid, dash, and dash–dot lines correspond to lattice matched, compressively strained, and tensile strained layers, respectively.

under one order of magnitude although the hole concentration is one order of magnitude higher. Finally, in Fig. 5, the absorption coefficients of the layers with a hole concentration of 10^{19} cm^{-3} are plotted. The absorption increase is, on average, 6× higher despite the fact that the free-hole concentration is 10× higher in this case, which shows that the absorption saturation has occurred for this hole concentration. Another observation is that, in the case of the x polarization, the absorption difference between the compressively strained layer and the other two layers is lower for this hole concentration.

B. Split-off to heavy and light hole transitions

In Figs. 6 and 7, the absorption coefficients for the split-off band to heavy and light hole bands are shown. The results are only for hole concentrations of 10^{17} and 10^{19} cm^{-3}. The results for a hole concentration of 10^{18} cm^{-3} are the same as those in the case of 10^{17} cm^{-3}, except for an order-of-magnitude higher absorption coefficients in the former case. The Fermi–Dirac distribution function at 300 K has a relatively large transition from 1 to 0 and many of the electronic states in the light hole band are also not occupied with electrons and therefore the split-off band to light hole band transition is not negligible for lower energies. When the photon energy increases, the absorption coefficient drops quickly because the effect of the increase in the momentum matrix element and the joint density of states is smaller than the effect of the decrease in the Fermi–Dirac distribution function. For the split-off band to heavy hole band transition, this is not the case and the absorption coefficient increases in the range of the energy shown in the figure. One, however, should note that at higher photon energies, the effect of the latter will be more dominant and hence this absorption will decrease with increasing energy.

As can be seen from the figure, the split-off band to light hole band absorption coefficient is stronger in the case of the x polarization, with the highest peak being for the lattice matched layer. In the z-polarization case, the compressively strained layer shows the largest peak of absorption. For the split-off band to heavy hole band transition, the absorption is stronger in the case of the z polarization. While in the case of the z polarization, the absorption coefficient for all three layers is almost the same, in the case of the x polarization, the difference between the lowest and highest absorption coefficient on average is about a factor of 2. Among the two strained layers, for the split-off band to light hole band (the split-off band to heavy hole band) transition, the absorption is stronger in the compressively strained layer in the case of the z polarization (x polarization), and in the tensile strained layer in the case of the x polarization (z polarization).

For a free-hole concentration of 10^{19} cm^{-3}, the number of empty electronic states in the light hole band is much higher and therefore the split-off band to light hole band absorption is greatly enhanced (see Fig. 7), more than two

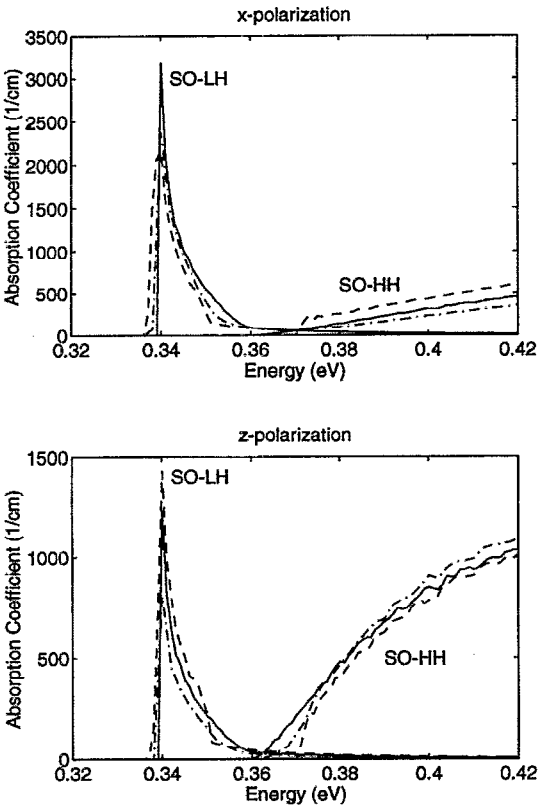

FIG. 7. Split-off band to light and heavy hole bands absorption coefficients for 10^{19} cm^{-3} free-hole concentration at 300 K for both x and z polarizations. Solid, dash, and dash–dot lines correspond to lattice matched, compressively strained, and tensile strained layers, respectively.

orders of magnitude, while the hole concentration is two orders of magnitude higher. The split-off band to heavy hole band absorption coefficient is also higher in this case but less than two orders of magnitude which represents the absorption saturation for this transition.

V. SUMMARY

The purpose of this work was to study the effects of the biaxial strain on the intervalence-band absorption spectra of p-doped bulk layers. The material system used in our calculation was the InGaAs/InP system for which we carried out the calculations for two strained layers (one under the compressive strain and the other under the tensile strain) and compared the results with those of the lattice matched layer. The $\mathbf{k}\cdot\mathbf{p}$ Hamiltonian was used to calculate the valence-band structure and the momentum matrix elements for these layers. The matrix elements were used to calculate the oscillator strengths which were strong functions of the polarization and the wave vector. To determine the intervalence-band absorption coefficients accurately, the calculation of the bandstructure and the oscillator strengths were performed for all the directions in phase space. Then the intervalence-band absorption coefficients for heavy hole band to light hole band, split-off band to heavy hole band, and split-off band to light hole band transitions for all three layers were carried out and compared. The effects of the biaxial strain on the intervalence-band absorption coefficients were different depending on the polarization, the strain type (compressive or tensile), and the valence bands involved in the transition. The threshold energy and the strength of absorption for the intervalence-band transitions were affected by the biaxial strain in the layer. The intervalence-band absorption in general increased with increasing the free-hole concentration.

ACKNOWLEDGMENTS

This work was supported by the NASA Center for Space Terahertz Technology under Contract No. NAGW-1334 and the Army Research Office–URI Program under Contract No. DAAL03-92-G-0109.

[1] A. H. Kahn, Phys. Rev. **97**, 1647 (1955).
[2] E. O. Kane, J. Phys. Chem. Solids **1**, 82 (1956).
[3] R. Braunstein, J. Phys. Chem. Solids **8**, 280 (1959).
[4] R. Braunstein and E. O. Kane, J. Phys. Chem. Solids **23**, 1423 (1962).
[5] G. S. Hobson and E. G. S. Paige, in Proceeding of the International Conference on the Physics of Semiconductors, Paris, 1964 (unpublished).
[6] J. B. Arthur, A. C. Baynham, W. Fawcett, and E. G. S. Paige, Phys. Rev. **152**, 740 (1966).
[7] I. Basiev, Phys. Rev. **177**, 1173 (1969).
[8] F. Keilmann, IEEE J. Quantum Electron. **12**, 592 (1976).
[9] R. B. James and D. L. Smith, Phys. Rev. B **21**, 3502 (1980).
[10] M. L. Huberman, A. Ksendzov, A. Larsson, R. Terhune, and J. Maserjian, Phys. Rev. B **44**, 1128 (1991).
[11] I. V. Altukhov, M. S. Kagan, K. A. Korolov, V. P. Sinis, and F. A. Smirnov, Sov. Phys. JETP **74**, 404 (1992).
[12] A. Afzali-Kushaa, G. I. Haddad, and T. B. Norris, *IEEE/Cornell University Conference on Advanced Concepts in High Speed Semiconductor Device and Circuits*, Virginia, 1993 (IEEE, Piscataway, NJ, 1993), 167–176.
[13] J. M. Luttinger and W. Kohn, Phys. Rev. **97**, 869 (1955).
[14] J. Singh, *Physics of Semiconductors and their Heterostructures* (McGraw-Hill, New York, 1993).
[15] Gennadii Levikovich Bir, Gennadii Levikovich, *Symmetry and Strain-Induced Effects in Semiconductors* (Wiley, New York, 1974).
[16] A. Afzali-Kushaa, Ph.D. dissertation, University of Michigan, 1994.
[17] Y. C. Chang and R. B. James, Phys. Rev. B **39**, 12672 (1989).